ELSEVIER

Polymer Vol. 37 No. 10, pp. 1775–1786, 1996

0032-3861/96/$15.00+0.00

Molecular theoretical study of the intimate relationships between structure and mechanical properties of polymer crystals

Kohji Tashiro* and Masamichi Kobayashi
Department of Macromolecular Science, Faculty of Science, Osaka University, Toyonaka, Osaka 560, Japan
(Received 15 May 1995)

Intimate relationships between the structure and the mechanical properties of polymer crystals are discussed from the molecular theoretical point of view. (1) The Young's modulus along the chain axis is dependent largely on the molecular conformation and the force constants. Some typical polymers including polyethylene, polyoxymethylene, poly(*p*-phenylene benzobisoxazole) and cellulose are discussed. (2) Three-dimensional anisotropy of the Young's modulus is discussed in relation to the packing mode of the chains. In the case of isotactic polypropylene crystal, the important role of anharmonic torsional vibrational modes of the methyl groups is discussed, which significantly governs the anisotropy of the elastic constants. (3) The molecular deformation mechanism was predicted lattice-dynamically and proved experimentally on the basis of vibrational spectroscopic measurements. The direct experimental evaluation of the theoretically predicted atomic displacements was performed for the first time through the refined X-ray structural analysis of polydiacetylene single crystal under the application of tensile stress. (4) The molecular design of novel polymer materials with three-dimensionally high Young's moduli is made starting from the various types of conventional polymer crystals such as poly(*p*-phenylene benzobisoxazole), polyacetylene, poly(*p*-phenylene), orthorhombic polyethylene and cellulose. Some of these crosslinked polymer crystals were found to possess a Young's modulus exceeding that of diamond crystal. Copyright © 1996 Elsevier Science Ltd.

(Keywords: polymer crystals; molecular theory; mechanical properties)

INTRODUCTION

Recently, remarkable developments have been attained for the so-called ultra-high-modulus fibres. In these materials the polymer chains are arrayed in parallel with a quite high degree of orientation along the draw axis, and the degree of crystallinity is also very high. In the limiting case the whole sample will become purely crystalline and so the mechanical properties intrinsic to the polymer crystal will appear directly as the bulk properties. As currently understood, it is very important to evaluate the intrinsic mechanical properties of the crystalline phase of polymers as exactly and quantitatively as possible. Data thus obtained of the limiting mechanical property must be interpreted well enough in connection with the molecular and crystal structures, from which the various important factors governing the mechanical properties should be extracted. These important factors will help us to produce novel polymer materials with excellent mechanical properties.

In the first part of this paper, an evaluation of the limiting elastic constants of polymer crystals will be reviewed briefly[1,2] in connection with the conformation and force constants of the polymer chains. These limiting mechanical properties can be correlated directly with the deformation mechanism of polymer crystals subjected to an external force field. In the second part of this paper, the theoretical and experimental techniques to trace the molecular deformation process will be described. In particular, the result of detailed X-ray structural analysis for polydiacetylene single crystal subjected to external tensile stress will be reported. This is the first direct experimental proof of the theoretically predicted atomic displacements induced by the tensile deformation of polymer crystals[3]. In the last section, molecular design of novel polymers with extremely high Young's modulus, which exceeds even that of diamond crystal, will be reported[4,5].

* To whom correspondence should be addressed

THEORETICAL APPROACHES TO CALCULATE THE ELASTIC CONSTANTS OF POLYMER CRYSTALS

In the calculation of three-dimensional elastic constants of polymer crystals, we have employed three types of theoretical approach.

One is the so-called lattice dynamical theory developed by Born[6]. The equation for the elastic constant tensors is derived by assuming that the strain energy of the polymer crystal becomes minimal with respect to the atomic displacements induced by external stress. The elastic constants are calculated according to the following equation:

$$\boldsymbol{c} = (1/v)[\boldsymbol{F}_{\sigma} - \tilde{\boldsymbol{F}}_{\rho\sigma}(\boldsymbol{F}_{\rho})^{-1}\boldsymbol{F}_{\rho\sigma}] \quad (1)$$

where v is the volume of the unit cell and $\boldsymbol{F}_\sigma$, $\boldsymbol{F}_{\rho\sigma}$ and $\boldsymbol{F}_\rho$ are the matrices constructed by the atomic coordinates, $\boldsymbol{B}$ matrix (the transformation matrix between the Cartesian displacement coordinates and the internal displacement coordinates) and force-constant matrix $\boldsymbol{F}$. On the other hand, the normal vibrational frequencies ν can be calculated by the following dynamical equation:

$$|\tilde{\boldsymbol{M}}^{-1/2}\tilde{\boldsymbol{B}}\boldsymbol{F}\boldsymbol{B}\boldsymbol{M}^{-1/2} - \lambda\boldsymbol{E}| = 0 \qquad (2)$$

where $\boldsymbol{B}$ and $\boldsymbol{F}$ are the same as defined above, $\boldsymbol{M}$ is the matrix of atomic masses, λ are the eigenvalues and $\boldsymbol{E}$ is the identity matrix. As seen in equations (1) and (2), the vibrational frequencies and elastic constants can be calculated simultaneously using a set of structural parameters and force constants. In other words, we may obtain reasonable calculated elastic constants by using the $\boldsymbol{B}$ and $\boldsymbol{F}$ matrices checked by a comparison of observed and calculated vibrational frequencies. When the calculation is attempted for a polymer crystal with a complicated structure, however, the preparation of the input data is quite cumbersome and so careless mistakes can occur frequently. In addition, large memory size is needed for the computer and the calculation speed becomes very slow. By utilizing the symmetry relation of the polymer crystal, equations (1) and (2) become simpler, making application easier to complicated polymer crystals, because only data concerning the crystallographically asymmetric unit are necessary in the calculation[7]. The lattice dynamical theory can be developed further by introducing anharmonic potential functions under the quasiharmonic approximation, and the elastic constants (and lattice vibrations) can be calculated as functions of temperature and stress[8–11].

The second approach is the so-called molecular mechanics method[12]. The potential energy V is developed with respect to the external strain ϵ_{ij} as:

$$V = V_0 + \sum_{ij}(\partial V/\partial\epsilon_{ij})_0\epsilon_{ij} + \frac{1}{2}\sum_{ij}\sum_{kl} \times (\partial^2 V/\partial\epsilon_{ij}\partial\epsilon_{kl})_0\epsilon_{ij}\epsilon_{kl} + \ldots \qquad (3)$$

The second derivatives $(\partial^2 V/\partial\epsilon_{ij}\partial\epsilon_{kl})_0$ correspond to the elastic constants c_{ijkl}. In the actual calculation we utilized the commercially available program 'Professional Polygraf' (Molecular Simulations Inc., USA).

The third method is to utilize the molecular dynamics technique as developed by Rahman *et al.*[13], in which the fluctuation of internal strain (or stress) is related to the elastic constants. We applied this method to evaluate the temperature dependence of Young's modulus of polyoxymethylene crystal, as will be described in a later section.

STRUCTURE AND MECHANICAL ANISOTROPY OF POLYMER CRYSTALS (BRIEF REVIEW)[1,2]

Chain conformation and Young's modulus

Owing to the characteristic structure of polymer crystals in which the molecular chains constructed by covalent bonding are packed together by weak non-bonded intermolecular interactions, the mechanical anisotropy of polymer crystals is very high; the Young's modulus E_c along the chain axis is 1–2 orders of magnitude higher than those in the directions perpendicular to the chain axis. Therefore, as an approximation, the Young's modulus predicted for an isolated single chain may be a good measure for the limiting modulus of the polymer crystal along the chain axis. At the present stage we can say that the intimate relationship between E_c and the chain conformation is well enough understood theoretically; in other words, the modulus of a chain can be predicted quantitatively as long as the chain conformation is reasonably constructed. In this section we will discuss the intimate relationship between the structure and Young's modulus for many types of polymers and extract the factors governing the Young's modulus of chains. Of course, the modulus must be evaluated originally by taking both the intra- and intermolecular interactions into consideration. In some examples here, the modulus contains contributions from both of these interactions.

Planar-zigzag conformation. When a tensile force is applied to the planar-zigzag polyethylene (PE) chain[14], the strain energy distributes to the skeletal CC bond stretching and CCC bond angle deformation by about 50% each, as shown in *Figure 1*. This is the reason why the PE modulus is as high as 300 GPa. The modulus of planar-zigzag poly(vinyl alcohol) (PVA), ca. 287 GPa, is also in this order of magnitude, although the larger cross-sectional area reduces the modulus slightly compared with the modulus of PE chain[14]. The molecular conformation of α-form nylon-6 has been proposed to be planar-zigzag. But the crystallite modulus measured at room temperature is only 100 GPa[15], far below the value predicted theoretically for the planar-zigzag chain structure. Recent studies revealed that this polymer chain experiences a thermal motion at room temperature and contracts to some extent from the planar-zigzag conformation. As the temperature decreases to liquid-nitrogen temperature, the repeating period of the chain increases and approaches the value intrinsic to the extended zigzag form[15]. Correspondingly, the crystallite modulus increases to 270 GPa at liquid-nitrogen temperature, the value predicted for the planar-zigzag structure. The lattice dynamical calculation showed the high sensitivity of the modulus to the slight contraction of the chain: the calculated E_c decreases drastically from ca. 300 to 100 GPa when the chain is contracted by only 0.6% from the planar-zigzag conformation through the torsional mode around the amide–methylene bonds (*Figure 2*)[16].

Helical and glide-plane-type chains. Polyoxymethylene (POM) is a typical helical chain consisting of a sequence of *gauche* C–O bonds. The strain energy distributes mainly to the bond angle deformation and internal twisting of these bonds (*Figure 1*). The calculated modulus is 109 GPa, which is in good agreement with the modulus of about 105 GPa obtained experimentally at −150°C[17]. Isotactic polypropylene (i-PP) is another example of the helical chain conformation. The theoretical value of 40 GPa[11] agrees well with the X-ray observed value, ca. 40 GPa[18]. The strain energy distributions to the internal twisting and the bond angle deformation of the skeletal chain are large and the CC stretching modes also contribute to some extent in this case because of the characteristic *TGTGTG*... conformation. Poly(ethylene

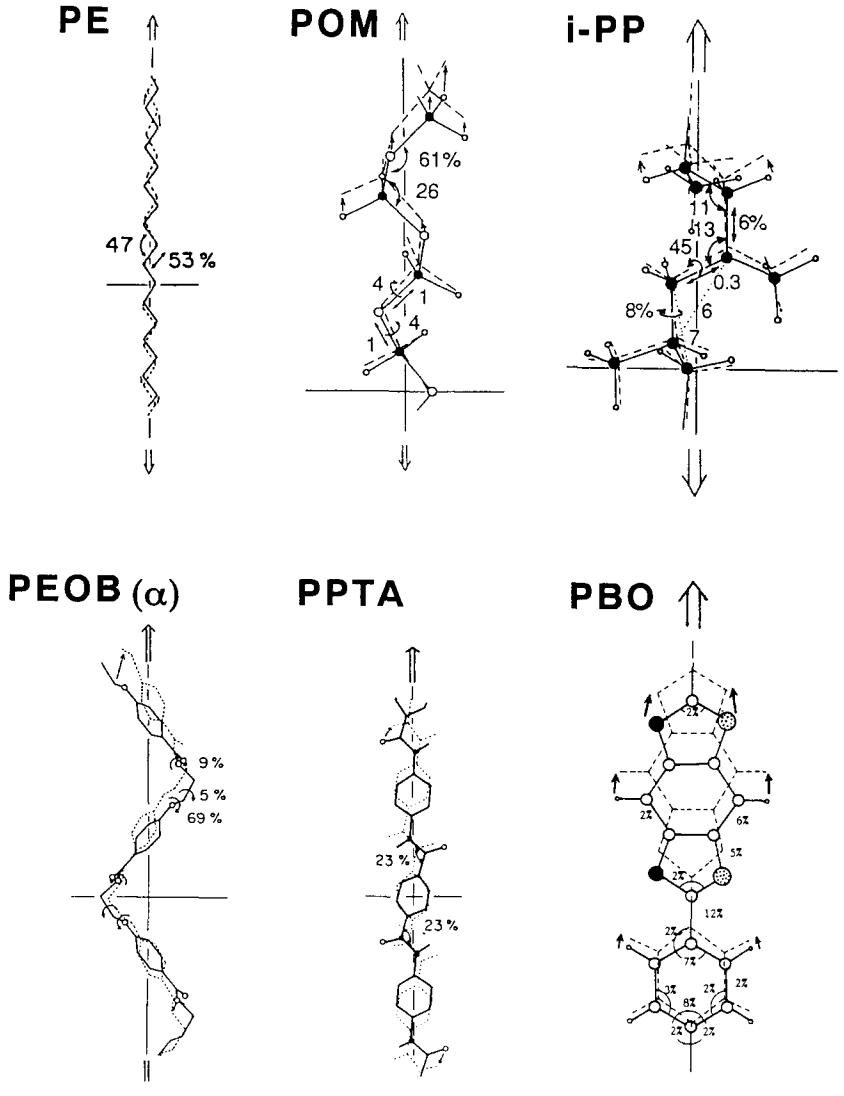

Figure 1 Molecular deformation mechanism and strain energy distribution calculated for various polymer chains subjected to a hypothetically large strain of 10%

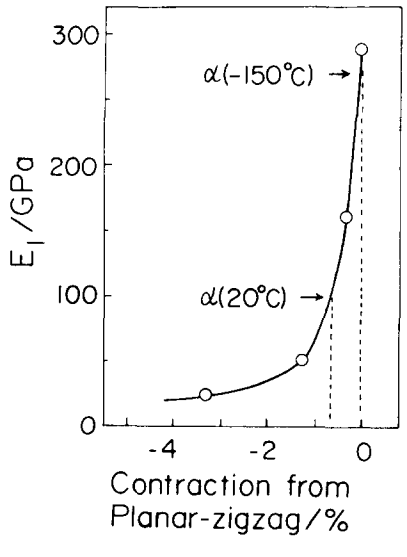

Figure 2 The Young's modulus along the chain axis of α-form nylon-6 calculated as a function of the degree of contraction of the chain from the planar-zigzag conformation. The arrows indicate the values measured by the X-ray diffraction method at various temperatures[15] (from ref. 16)

oxybenzoate) (PEOB, $-(OCH_2CH_2OCOPh)-$) has two types of chain conformation in the crystalline lattice. The α form is a zigzag-type helix with very long arms of monomeric unit[19] and the chain is deformed easily through internal twisting around the sequence of $C(Ph)-O-CH_2-CH_2-C(O)$: about 85% of the total strain energy distributes to this internal twisting coordinate as shown in *Figure 1*. Thus the limiting modulus of the α form is only 2 GPa (calculated)[20] or 6 GPa (X-ray value)[21]. In contrast, the modulus of another crystal modification, the β form, is calculated to be ca. 57 GPa[20]. The β form takes the fully extended planar-zigzag conformation[22] and the strain energy does not distribute to the internal rotations but mostly to bond angle deformation of the skeletal chain. This large difference in the modulus between the α and β forms is a good example of the high sensitivity of the Young's modulus to conformational differences of the polymer with the *same* chemical formula.

Rigid-rod polymers. The poly(*p*-phenylene terephthalamide) (PPTA) chain is fully extended and consists of an alternation of rigid aromatic rings and

amide groups. The chain conformation may be assumed as a kind of planar-zigzag form consisting of the alternation of short and long linear bonds that correspond to the amide C(O)–N bond and *p*-substituted phenylene ring, respectively. These virtual bonds tilt to some extent from the vertical axis of the chain and so the strain energy distributes mainly to the deformation of the bond angles of the zigzag chain (*Figure 1*), resulting in a Young's modulus that is not so high as expected from the chemical formula of the rigid amide and phenylene groups, but is only 182 GPa (calculated)[20] and 200 GPa (observed)[23]. In other words, the rigidity of aromatic groups is not reflected effectively in the modulus of the PPTA chain. Poly(ethylene terephthalate) (PET) has a situation similar to that of PPTA. The Young's modulus is only ca. 95 GPa[20]. The crystallite modulus measured by the X-ray method is 110 ± 10 GPa[24,25], which is in good agreement with the calculated value.

Poly(*p*-phenylene benzobisthiazole) (PBT) and poly(*p*-phenylene benzobisoxazole) (PBO) are typical rigid-rod polymers and exhibit the highest bulk tensile moduli among the various synthetic polymers:

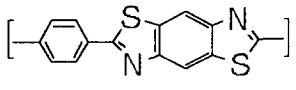

PBT

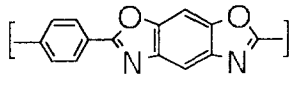

PBO

The lattice-dynamically calculated Young's moduli of PBT and PBO are 405 and 460 GPa, respectively[26]. These calculated moduli are in good agreement, respectively, with the X-ray values of 395 and 477 GPa measured by Lenhert and Adams[27]. The crystallite modulus of PBT was measured also by Nakamae *et al.* to be ca. 372 GPa[39]. As shown in *Figure 1*, the strain energy distributes to the internal deformation of the phenylene and heterocyclic rings as well as to the stretching of the linkages connecting these two rings. The strain energy distribution to the torsional coordinates around these linkages is almost zero, indicating no contribution of such torsional modes to the Young's modulus. Wierschke *et al.* evaluated the Young's modulus of PBT and PBO to be 620 and 690 GPa, respectively, on the basis of the semiempirical molecular-orbital method (Austin model 1, AM1)[28]. These values seem to be overestimated, as stated by the authors themselves. Poly(*p*-phenylene pyromellitimide) (PPPI) is a perfectly linear polymer, giving the calculated modulus of 505 GPa[29]. Poly(*p*-phenylene) (PPP) is also a linear polymer having a 1,4-linkage of benzene rings, and the calculated modulus is 275 GPa:

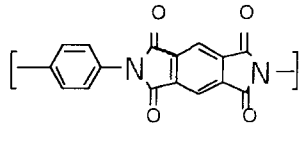

PPPI

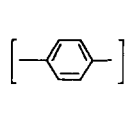

PPP

Cellulose. A sheet of paper, made of cellulose, is very stiff, as is well known in our everyday life (for example, you may have had the experience of having your fingers cut by paper). The crystallite modulus of native cellulose (cellulose I) measured by X-ray diffraction is 120–140 GPa and that of regenerated cellulose (cellulose II)

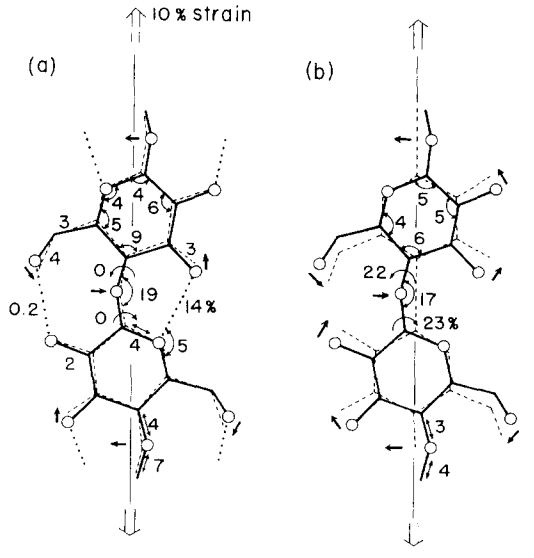

Figure 3 Tension-induced molecular deformation and the corresponding strain energy distribution calculated for the cellulose chain (a) with and (b) without intramolecular hydrogen bonds (from ref. 32)

is 90–112 GPa[30,31]. The high Young's modulus of the cellulose chain was identified to originate from the role of intramolecular hydrogen bonding[32]. The calculation of the modulus was made by neglecting the various intermolecular and intramolecular interactions one at a time, step by step. The modulus is not affected significantly even when all the intermolecular interactions are neglected. But a deletion of intramolecular hydrogen bonds was found to give a modulus only about 40% of the original modulus obtained with all the inter- and intramolecular interactions taken into account. This remarkable reduction of the modulus can be interpreted reasonably by investigating the strain energy distribution, as shown in *Figure 3*. Ignoring intramolecular hydrogen bonds induces easy internal twisting around the inter-ring ether linkages when the chain is stretched (*Figure 3b*). This chain deformation through internal twisting is prevented when intramolecular hydrogen bonds are introduced; i.e. chain deformation occurs via bond angle deformation of the ether linkage, intra-ring deformation and stretching of the hydrogen bonds (*Figure 3a*). This molecular deformation mechanism results in the high Young's modulus of the cellulose chain.

Anisotropy of elastic constants in planes perpendicular to the chain axis

Anisotropy of the elastic constants relates intimately to the three-dimensional packing structure of polymer chains in the crystal lattice. In the orthorhombic PE crystal, for example, the non-bonded interatomic interactions are important, which work effectively in all the lateral directions. As a result the Young's modulus and linear compressibility are almost isotropic in the *ab* plane, although the *a* axis is a little softer than the *b* axis (*Figure 4*)[14]. PVA is more rigid in the lateral directions, originating from a network structure constructed by the intermolecular hydrogen bonds[14]. A similar situation is also seen for cellulose II and poly(*m*-phenylene isophthalamide) (PPIP)[32]. In the unit cell of cellulose II, the chains are linked by intermolecular hydrogen bonds in

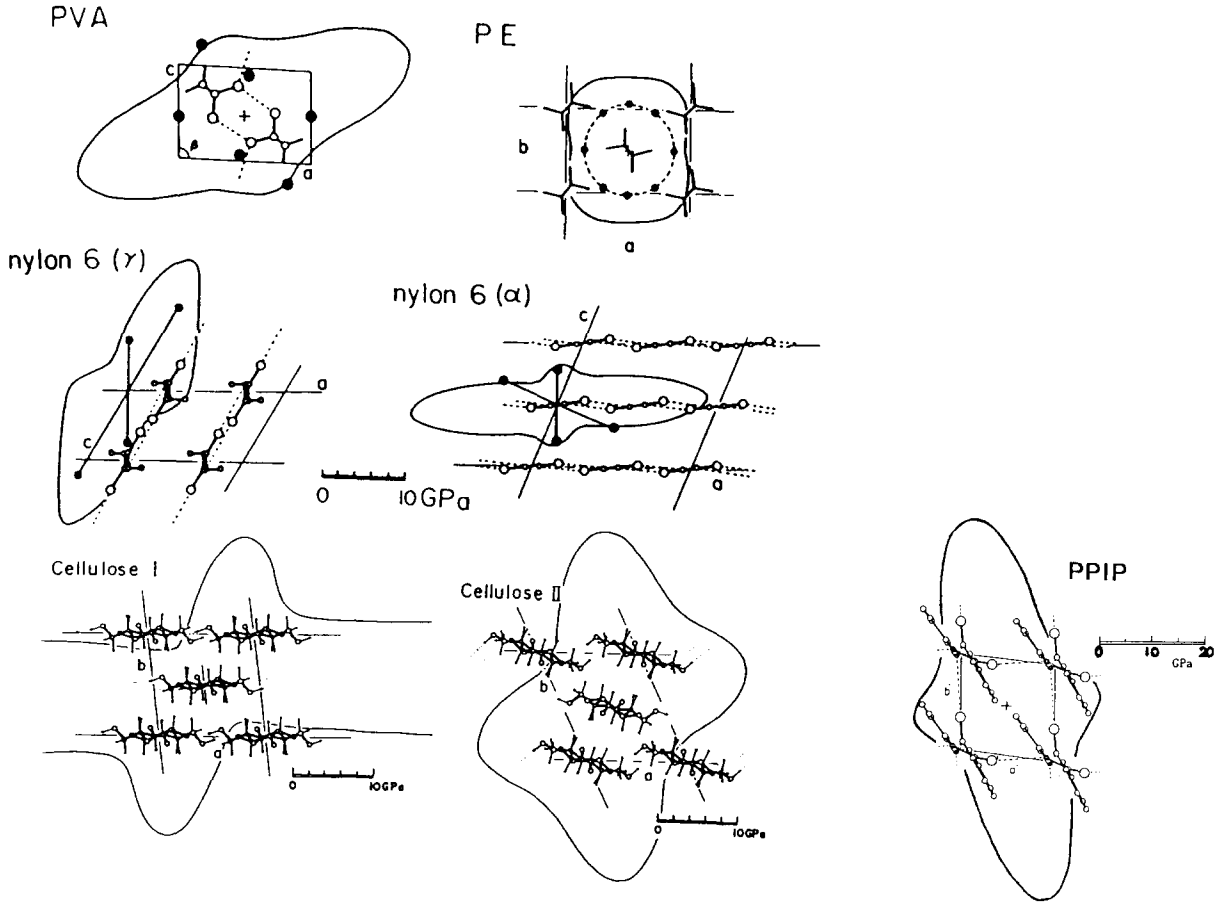

Figure 4 Anisotropy of the Young's modulus in the plane perpendicular to the chain direction. The full circles are the data observed by X-ray diffraction

all three directions. In the case of PPIP crystal, the intermolecular hydrogen bonds are also made along the *a* and *b* axes just like a jungle gym (*Figure 4*), where the *c* axis is along the chain direction[32]:

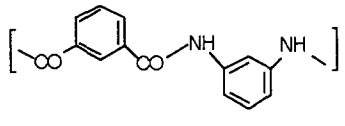

Nylon-6 α and γ forms[16] and cellulose I[32] show significantly large anisotropy of the Young's modulus and linear compressibility in the planes perpendicular to the chain axis. The molecular chains are linked by intermolecular hydrogen bonds to form a sheet structure and these sheets are stacked together by weak van der Waals interactions. The modulus in the sheet plane is several times higher than that in the direction perpendicular to the plane. By neglecting the intermolecular hydrogen bonds, the anisotropic curves change into isotropic form.

Characteristic behaviour is seen for the elastic modulus in the *ab* plane of i-PP crystal. This polymer has methyl groups that spread out from the skeletal chains just like branches of trees. Therefore the mechanical anisotropy is considered to be mostly governed by the intermolecular interactions between these methyl groups. The anisotropy of the Young's modulus and linear compressibility was calculated for i-PP crystal by taking all the methyl–methyl interactions into account[11]. But the observed anisotropy of the linear compressibility[33] was not reproduced well. The temperature dependence of the far-infra-red spectra of i-PP film revealed that the bands of methyl torsional modes ($\tau(CH_3)$) around 200 cm^{-1} change the profile remarkably as the sample is cooled from room temperature to liquid-nitrogen temperature, meaning that the methyl torsional modes are highly anharmonic. Then, as a measure of anharmonicity, the so-called mode Grüneisen constants γ of the $\tau(CH_3)$ modes were introduced into the equation for the three-dimensional elastic constants: the isothermal elastic constants c_{ij}^T are expressed approximately by the following equation[11]:

$$c_{ij}^T \approx c_{ij}^0 - kT \sum_l \gamma_{il}\gamma_{jl} \tag{4}$$

where c_{ij}^T and c_{ij}^0 are the elastic constants at temperature T and 0 K, respectively, and k is the Boltzmann constant. The mode Grüneisen constant γ_{il} is defined as $-(\partial\nu_l/\partial\epsilon_i)_0/\nu_l$ where ν_l is the vibrational frequency and ϵ_i is a strain. By substituting suitable values for the γs, the elastic constants were calculated to give a reasonable reproduction of the mechanical anisotropy measured at room temperature.

MECHANICAL DEFORMATION MECHANISM OF POLYMER CRYSTALS

As discussed in the previous sections, it is useful to interpret the limiting Young's modulus and three-

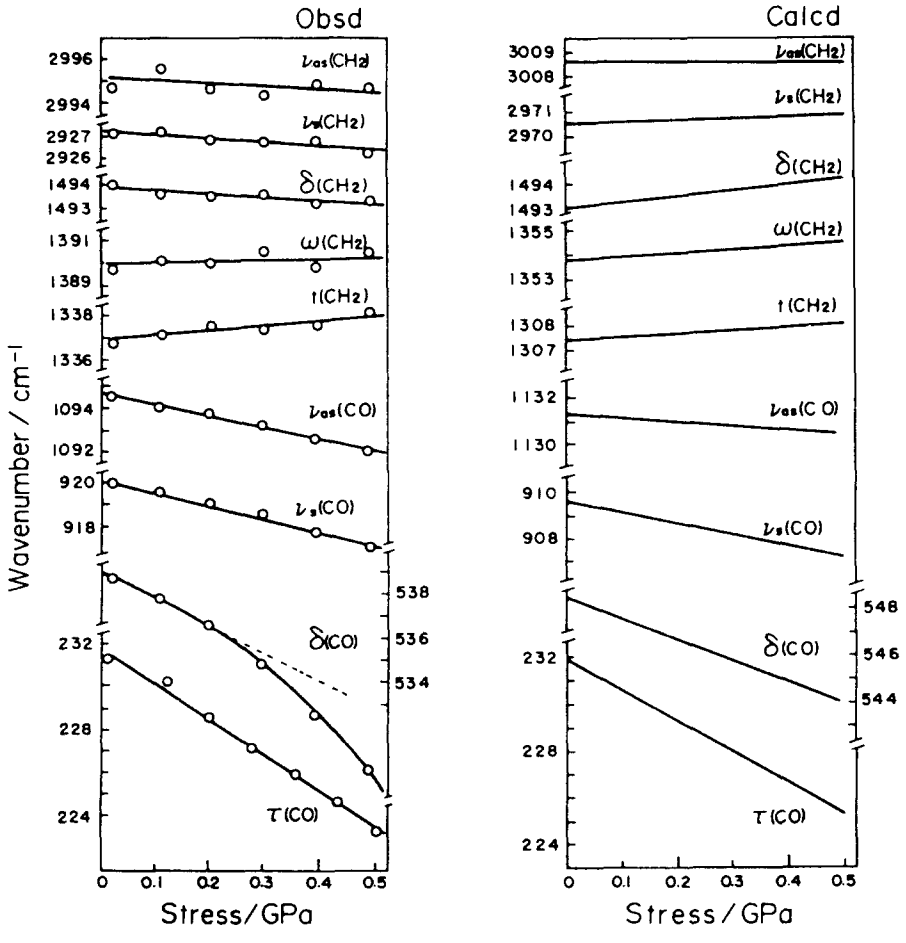

Figure 5 Observed and calculated vibrational frequencies as a function of tensile stress applied to the polyoxymethylene chain. $\nu_{as}(CH_2)$, $\nu_s(CH_2)$, $\delta(CH_2)$, $w(CH_2)$ and $t(CH_2)$ are the antisymmetric stretching mode, symmetric stretching mode, bending mode, wagging mode and twisting mode of the methylene group, respectively. $\nu_{as}(CO)$, $\nu_s(CO)$, $\delta(CO)$ and $\tau(CO)$ are the antisymmetric stretching mode, symmetric stretching mode, bending mode and torsional mode concerning the CO skeletal bonds, respectively (from ref. 9)

dimensional elastic constants of polymer crystals in terms of the strain energy distribution and the atomic displacements, in other words, on the basis of the molecular deformation mechanism. It is necessary, however, to confirm experimentally the theoretically predicted atomic displacements.

Vibrational spectroscopic method

Vibrational spectra are very sensitive to slight changes in local structure and therefore may be one of the most powerful methods to trace the stress-induced changes in structure and interactions. We measured the infra-red and Raman spectral changes induced by the application of tensile stress for various polymer samples, and interpreted the data on the basis of the atomic deformation mechanism predicted by the lattice dynamical theory.

For example, in the case of POM, a large low-frequency shift is seen for the vibrational bands of C–O stretching, C–O–C and O–C–O bending, and COCO torsion, as shown in *Figure 5*[17]. The bands of the CH_2 side groups do not shift at all or rather shift to the higher-frequency side (e.g. CH_2 twisting mode, $t(CH_2)$). This spectral change is consistent with the strain energy distribution calculated for this polymer chain (*Figure 1*). That is, the vibrational modes corresponding to the internal coordinates to which the strain energy preferentially distributes show large frequency shifts when the chain is tensioned.

What is the mechanism of these vibrational frequency shifts? The vibrational frequency shift can be reasonably understood as an anharmonic effect of the vibrations. In order to quantify this stress-induced vibrational frequency shift of polymer crystals, we have developed a lattice dynamical theory under the quasiharmonic approximation[8,9], where the potential energy V is:

$$V = V_0 + \sum_i \left(\frac{\partial V}{\partial R_i}\right)_0 \Delta R_i + \frac{1}{2}\sum_i \sum_j \left(\frac{\partial^2 V}{\partial R_i \partial R_j}\right)_0 \Delta R_i \Delta R_j + \frac{1}{6}\sum_i \sum_j \sum_k \left(\frac{\partial^3 V}{\partial R_i \partial R_j \partial R_k}\right)_0 \Delta R_i \Delta R_j \Delta R_k + \cdots$$

$$\approx \frac{1}{2}\sum_i \sum_j \left[\left(\frac{\partial^2 V}{\partial R_i \partial R_j}\right)_0 + \frac{1}{3}\sum_k \left(\frac{\partial^3 V}{\partial R_i \partial R_j \partial R_k}\right)_0 \Delta R_k\right] \times \Delta R_i \Delta R_j = \frac{1}{2}\sum_i \sum_j \left[f_{ij}^0 + \sum_k f'_{ijk} \Delta R_k\right] \times \Delta R_i \Delta R_j = \frac{1}{2}\sum_i \sum_j f_{ij} \Delta R_i \Delta R_j \quad (5)$$

In this way the potential energy can be expressed in a harmonic form but the force constants f_{ij} are affected by the change in the internal coordinate ΔR as defined by the equation $f_{ij} = f_{ij}^0 + \sum_k f'_{ijk} \Delta R_k$. The ΔR is

expressed as a function of the force constants, atomic coordinates of the initial structure and strain, and therefore f_{ij} is also expressed as a function of strain (or stress). By using these force constants, the vibrational frequency ν is calculated as a function of the strain on the basis of equation (2). This idea was formulated and applied to several cases including PE, POM and i-PP[8,9]. In *Figure 5* the vibrational frequency shifts calculated for the POM chain are plotted against applied stress with good reproduction of the observed data.

In the above sections we pointed out the good correlation between the strain energy distribution and the vibrational frequency shift. Both terms can be connected reasonably in the following manner. The strain energy distribution (*SED*) for the internal displacement coordinate ΔR is defined simply as:

$$(SED) = f\Delta R^2 \Big/ \sum f\Delta R^2 \approx f^0\Delta R^2 \Big/ \sum f^0\Delta R^2 \propto f^0\Delta R^2$$

i.e.

$$\Delta R \propto [(SED)/f^0]^{1/2} \quad (6)$$

The vibrational frequency of the corresponding ΔR is given as follows:

$$\nu \propto B(f/m)^{1/2} = B[(f^0 + f'\Delta R)/m]^{1/2} \approx B[(f^0/m)]^{1/2}[1 + f'\Delta R/(2f^0)] \approx \nu_0[1 + f'\Delta R/(2f^0)] \quad (7)$$

where B is the so-called $\boldsymbol{B}$ matrix related to the geometry and m is the reduced mass. From equations (6) and (7), the vibrational frequency shift $\Delta\nu$ is expressed as follows:

$$\Delta\nu = \nu - \nu_0 \approx \nu_0 f'\Delta R/(2f^0) \approx \nu_0 f'[(SED)/f^0]^{1/2}/(2f^0) \propto B(f'/f^0)(SED)^{1/2} \quad (8)$$

This equation tells us that the vibrational frequency shift induced by the chain deformation is proportional to the square root of the strain energy distribution. This equation says also that both the geometrical factor (B) and the interaction factor (f) govern the frequency shift and that the balance (f'/f^0) between the anharmonic force constant f' and the harmonic force constant f^0 is important for $\Delta\nu$: even when f^0 is small or the coordinate R is soft, the vibrational frequency shift $\Delta\nu$ may be small if the anharmonic force constant f' is small.

Refined X-ray structural analysis of strained polymer crystal

Vibrational spectroscopy is a powerful tool to trace the mechanical deformation of polymer crystals as viewed from the molecular level. But the spectral data give relatively indirect information about deformation mechanisms. This results because the vibrational frequency is governed by the coupling between atomic coordinates and force constants. Therefore, information on the atomic displacements cannot be extracted separately from the interaction term. In order to obtain this geometrical information more directly and explicitly, one must carry out accurate X-ray structural analysis for the sample subjected to tensile force. Unfortunately, however, this is not practicable for most synthetic polymers because the X-ray diffraction data are quite poor: the reflections are very broad and the number is limited to several tens at most. One exception is the case of polydiacetylene, which polymerizes into a giant single crystal, several centimetres in length. Recently we

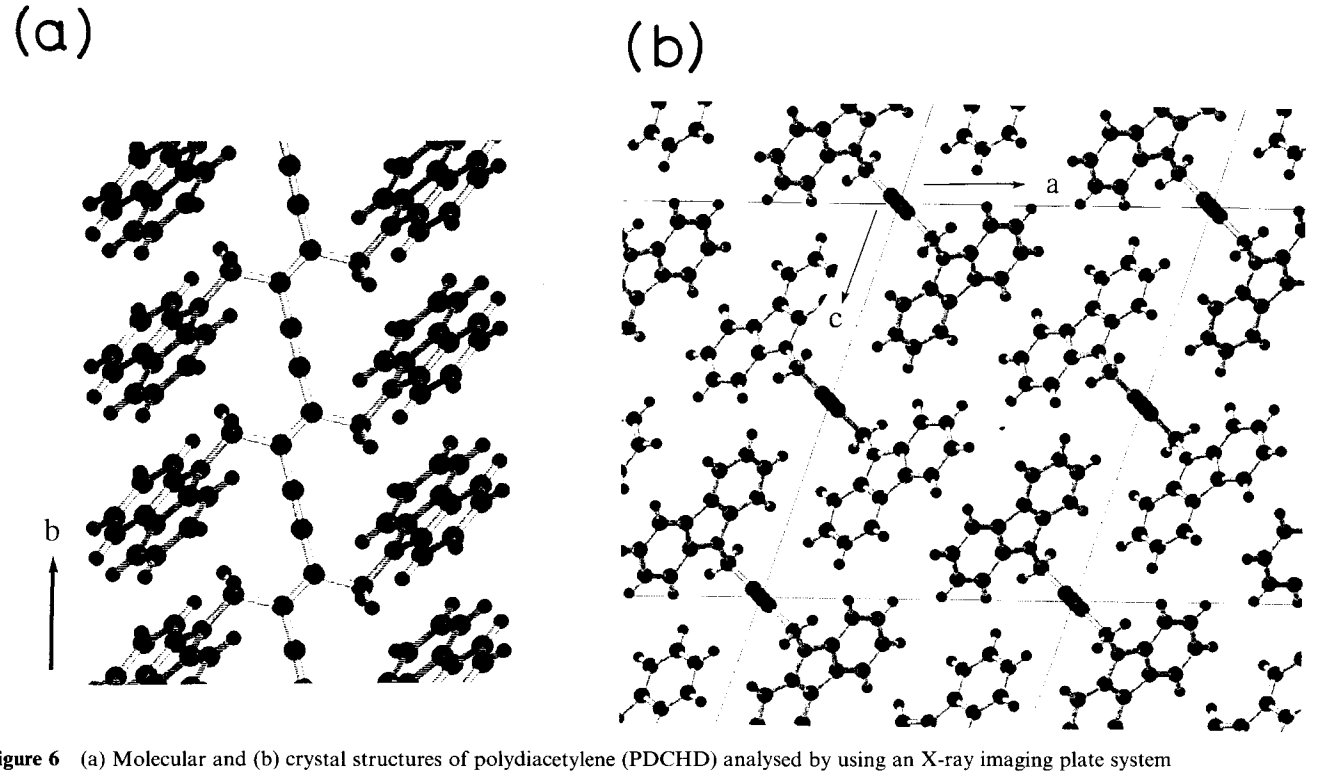

Figure 6 (a) Molecular and (b) crystal structures of polydiacetylene (PDCHD) analysed by using an X-ray imaging plate system

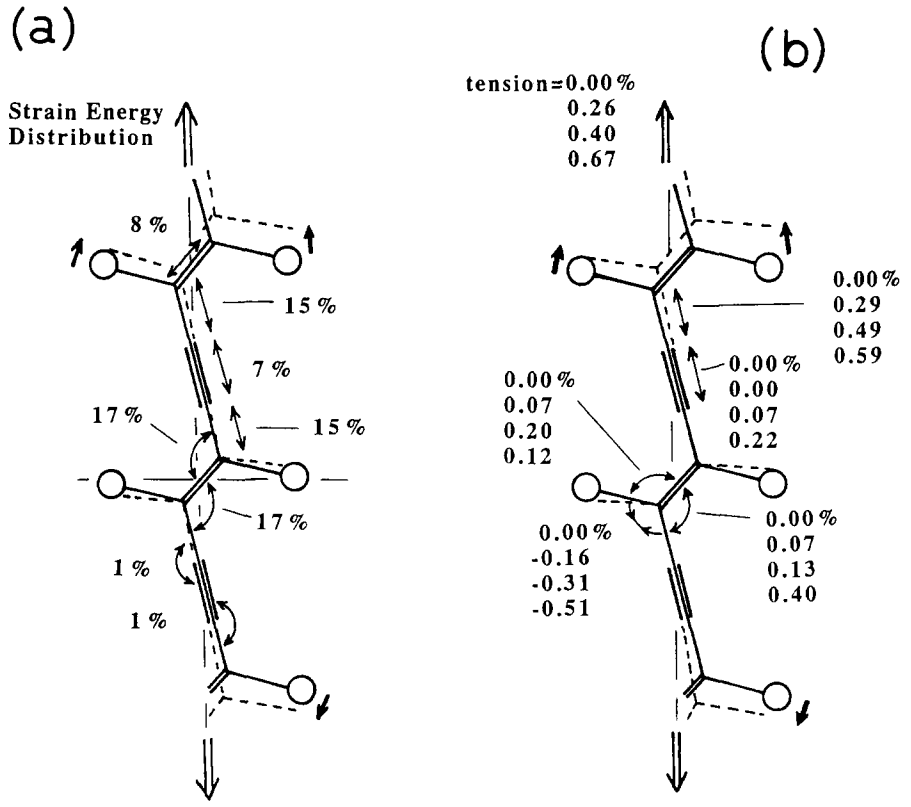

Figure 7 Molecular deformation mechanisms of polydiacetylene chain subjected to a tensile stress. (a) Lattice-dynamically predicted atomic displacements and strain energy distribution; (b) X-ray analysed changes of the internal coordinates. Each set of four figures denotes the percentage relative changes of each internal coordinate, corresponding to the four stages of the strain applied along the chain axis

succeeded in X-ray diffraction measurements of this polymer single crystal subjected to a constant tension and analysed the stress-induced atomic displacements directly[3].

The sample used for this experiment is poly[1,6-di(*N*-carbazolyl)-2,4-hexadiyne] (PDCHD) with the following chemical structure:

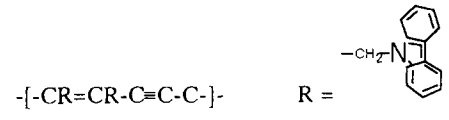

The sample was mounted in a home-made small stretcher, which was mounted on a goniometer head. Twenty shots of X-ray oscillation photographs (each oscillation angle 5° in the total range of 0–100°) were measured with the sample tensioned along the chain axis at a constant strain. The photographs were taken using an image plate (IP) system (DIP3000, Mac Science Co. Ltd, Japan). The total number of reflections collected from the set of 20 shots was about 6000. The collected data were analysed using the commercially available programs 'DENZO' (for the indexing of the reflections and the determination of the cell parameters) and 'Crystan GM' (for the direct method and the least-squares refinement of the strucure). In order to increase the experimental precision, about five samples were used for the independent sets of measurements at similar tensile strain and the results were averaged. In *Figure 6* is shown the molecular and crystal structure of PDCHD in the tensile-free state. *Figure 7* summarizes the structural changes of the PDCHD skeletal chain induced by the tensile strain, where the change in the internal coordinates (bond stretching, angle deformation, etc.) is shown as a percentage. The unit-cell parameters measured at each strain are listed in *Table 1*. The unit cell is stretched along the chain axis and contracts in the lateral directions with Poisson's ratio of ca. 0.7–0.4. As seen in *Figure 7b*, the C–C and C≡C bond lengths are stretched significantly and the angle C–C=C is increased and the angle R–C=C is decreased. These geometrical changes of the skeletal chain are quite consistent with the lattice-dynamically predicted atomic displacements shown in *Figure 7a*[34]. This may be the first successful experiment to prove the theoretically predicted chain deformation mechanism on the basis of a refined X-ray structural analysis. The details of the analysis will be published elsewhere.

Table 1 Unit-cell parameters of PDCHD at various strains

		Fibre axis		
Strain (%)	*a* (Å)	*b* (Å)	*c* (Å)	*β* (deg)
0.00	12.846	4.887	17.332	108.30
0.26	12.826	4.900	17.317	108.30
0.40	12.824	4.907	17.318	108.30
0.67	12.788	4.920	17.286	108.33

STRESS AND TEMPERATURE DEPENDENCES OF YOUNG'S MODULUS

As discussed in the previous section, nylon-6 α form shows a large temperature dependence of the crystallite

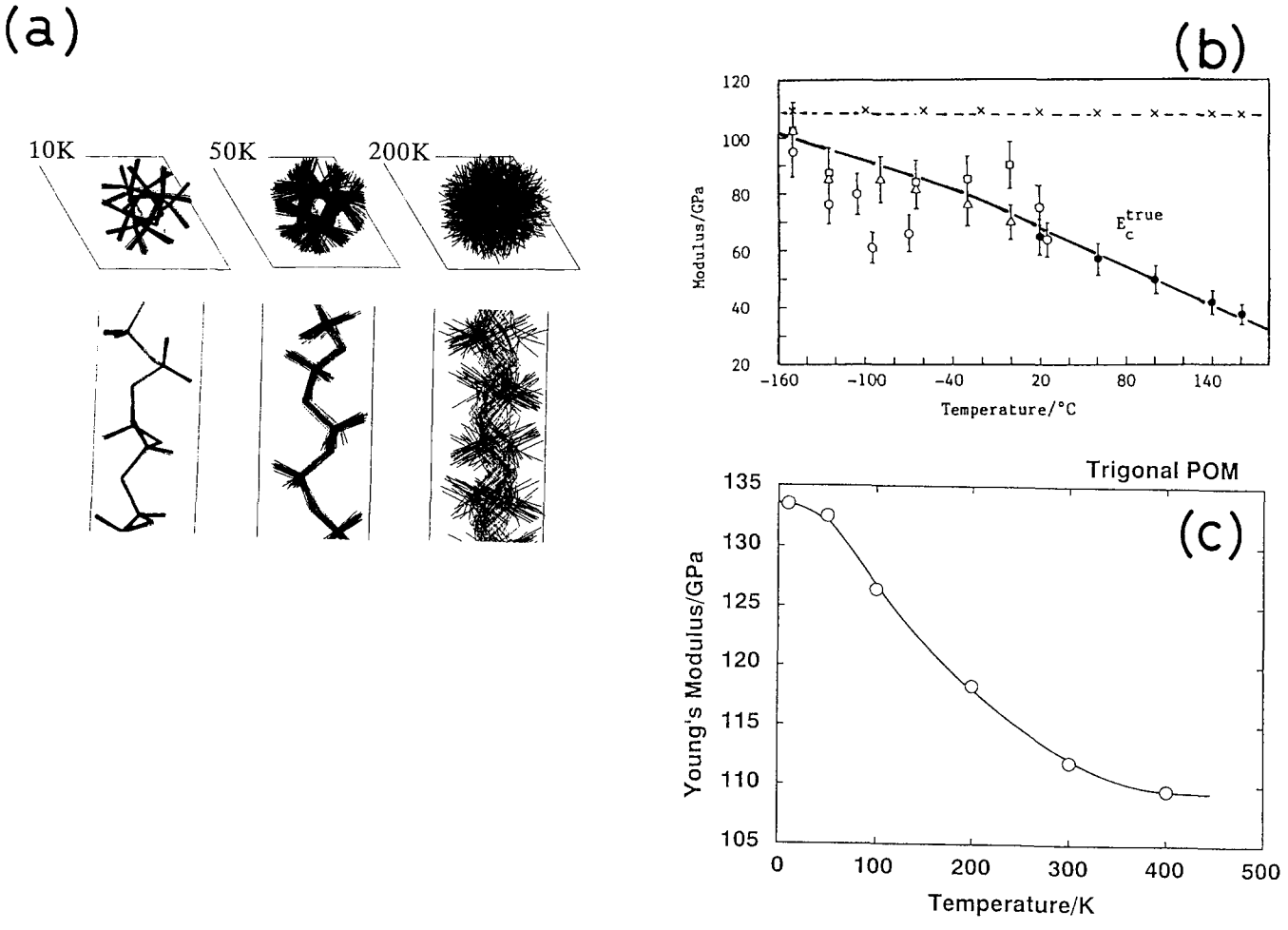

Figure 8 (a) Molecular motion of polyoxymethylene chain calculated by molecular dynamics. (b) Temperature dependence of the Young's modulus observed by the X-ray diffraction method (○, ●, □ and △). The crosses are the values calculated by lattice dynamics without any consideration of the large thermal motion of the chain[34]. (c) Temperature dependence of the Young's modulus calculated by molecular dynamics

modulus[15]: ca. 100 GPa at room temperature and 270 GPa at low temperature. This drastic change was attributed to the slight change in the chain conformation through the internal twisting motion around the skeletal bonds. This consideration was supported theoretically by the lattice-dynamical calculation[16].

The Young's modulus is dependent also on the externally applied stress. This originates from the anharmonic effect of the vibrations. This anharmonic effect can be detected by measuring the stress-induced vibrational frequency shift, as discussed in the previous sections. By introducing the force constants as a function of stress ($f = f^0 + f'\Delta R = f^0 + f''\sigma$), the Young's modulus can be expressed explicitly as a function of stress σ. For the POM model chain, the modulus E_c was approximately expressed as $E_c = 92.8 - 3.4\sigma$ (GPa), where the contribution of the anharmonic effect (the second term) is only ca. 4%[35].

Consideration of an anharmonic vibrational effect on the modulus also gives the temperature dependence of the modulus. The isothermal Young's modulus is approximately expressed as:

$$E_{iso}^T \approx E_{iso}^0 - kT\sum(\gamma_l)^2 \qquad (9)$$

where E_{iso}^0 is the modulus at 0 K and γ_l is a mode Grüneisen constant of the lth mode. The summation covers all the modes included in unit volume. For the POM chain, we estimate $E_{iso}^T \approx 109 - 0.045T$ (GPa)[35]. At $T = 300$ K, E_{iso} is 96 GPa, which is close to 75 ± 10 GPa measured by the X-ray method at room temperature. The molecular dynamics method gave the detailed temperature dependence of Young's modulus of POM[36]. In the calculation nine chains were packed into the cell and the time dependence of the unit-cell structure was calculated under conditions of constant temperature and pressure. As illustrated in *Figure 8a*, the chain experiences a rigorous thermal motion with increasing temperature and the conformation is more disordered, reflecting the large reduction of the modulus as shown in *Figure 8c*. This may be due to the coupling between the rotational motion of the chain with the internal twisting mode around the C–O skeletal bonds. The calculated temperature dependence of the modulus reproduces relatively well the X-ray observed data shown in *Figure 8b*[34]. The details will be published in a separate paper.

MOLECULAR DESIGN OF NOVEL POLYMER CRYSTAL WITH THREE-DIMENSIONALLY HIGH YOUNG'S MODULI

As discussed in the previous sections, rigid polymers such as PBO and PBT possess very high Young's modulus along the chain axis. However, one of their weak points

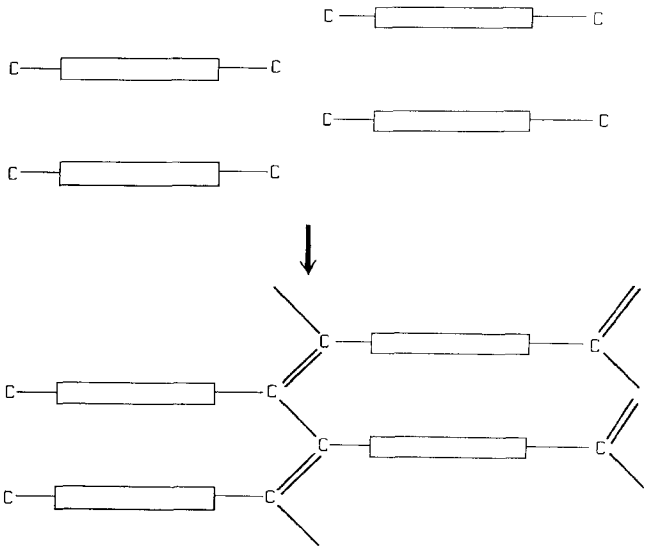

Figure 9 An illustration of the method to construct the three-dimensionally crosslinked network starting from the usual polymer crystal (from ref. 4)

lateral directions? One of the most effective methods may be the introduction of covalent crosslinks between adjacent molecular chains in the crystalline lattice. We tried to generate various types of crosslinks and found a simple but effective method of crosslinking[4]. As shown in *Figure 9*, the polymer chains are arrayed parallel to each other and the atoms (e.g. hydrogen atoms) extending from the main chains are replaced by carbon atoms, for example. These chains are shifted to positions suitable for the effective distances of crosslinking and then the carbon atoms of the side arms are covalently bonded between the adjacent chains by an alternate sequence of single and double bonds in a zigzag form. These crosslinked polymer lattices are energetically minimized and the three-dimensional elastic constant and compliance tensors are calculated. This method has been applied to PBO, poly(*p*-phenylene) (PPP) and polyacetylene (PA). For example, *Figure 10* shows the three-dimensionally crosslinked PA and PPP crystals. The calculated Young's moduli of the crosslinked polymers are listed in *Table 2*. These values were calculated by employing the universal force field[37]. The values are, of

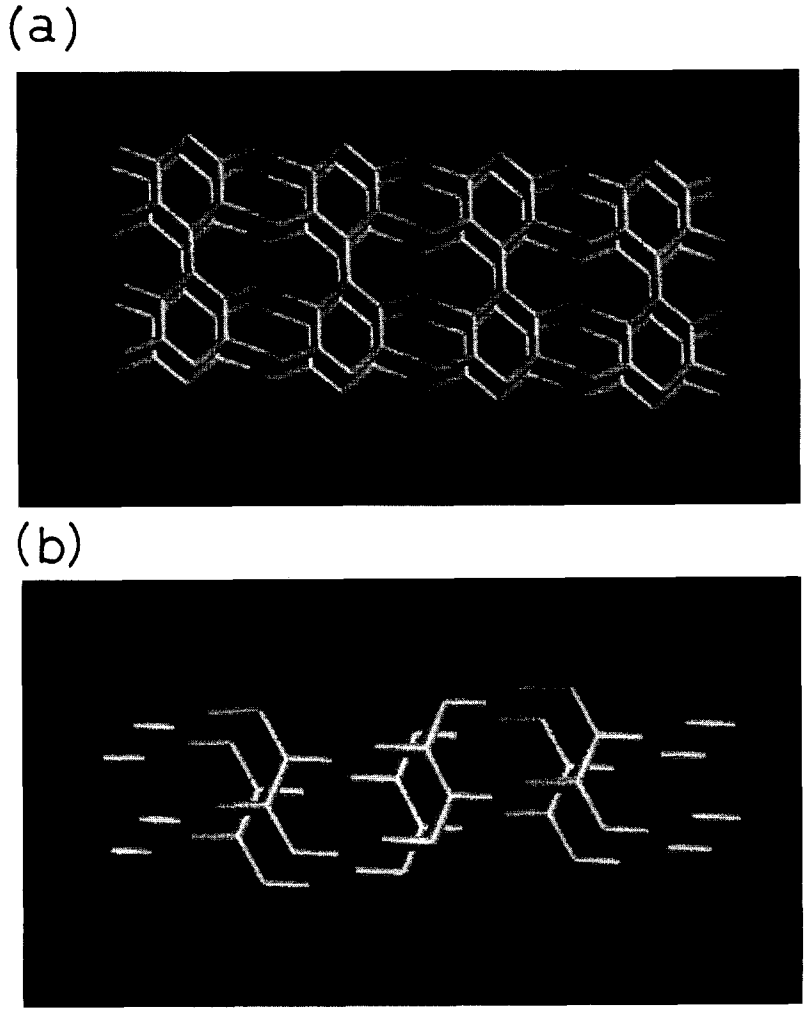

Figure 10 Three-dimensionally crosslinked polymer crystals: (a) poly(*p*-phenylene) and (b) polyacetylene

as structural materials is the low elastic modulus in the lateral directions, of the order of 10 GPa as calculated theoretically. How can we increase the moduli in the course, dependent on the force-field parameters utilized in the numerical calculation, but the essential points of the results are not changed. The modulus is in the range

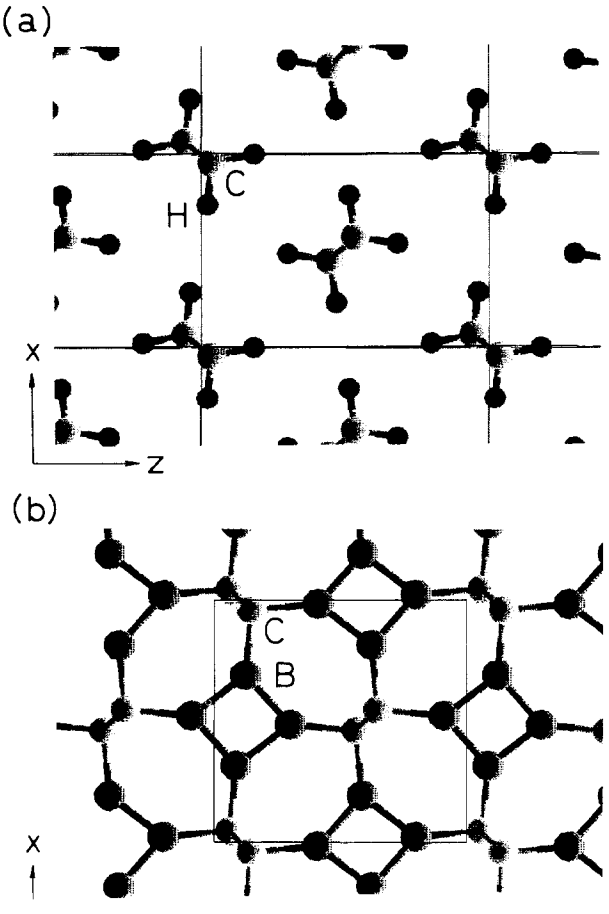

Figure 11 Structures of (a) orthorhombic polyethylene and (b) three-dimensionally crosslinked polyethylene crystals (from ref. 4). The hydrogen atoms in (a) are replaced by boron atoms in (b)

Table 2 Calculated Young's modulus of crosslinked polymer crystals

Crosslinked model	Axial modulus (GPa)	Lateral moduli (GPa)
PBO	873	665–712
PPP	1768	724–739
PA	1699	998–1796

Table 3 Young's moduli and bulk modulus (*BM*) for C_{60} and variously crosslinked C_{60} crystals

Model	Axial modulus (GPa)	Lateral moduli (GPa)	*BM* (GPa)
C_{60} simple cubic	36		27
1D polymer lattice	227	38, 45	37
2D network	231	52, 96	48
3D network	179	153, 153	107

of 700–1900 GPa in all three directions, which is close to or exceeds the Young's modulus of diamond crystal, ca. 1050 GPa calculated by using the same force-field parameters (the observed modulus is 1030 GPa).

This crosslinking method can be applied even to the case of orthorhombic polyethylene crystal as shown in *Figure 11*, where the hydrogen atoms are replaced by boron atoms and the *trans*-zigzag chains are linked by B–B bonds. For this crosslinked PE model, the modulus

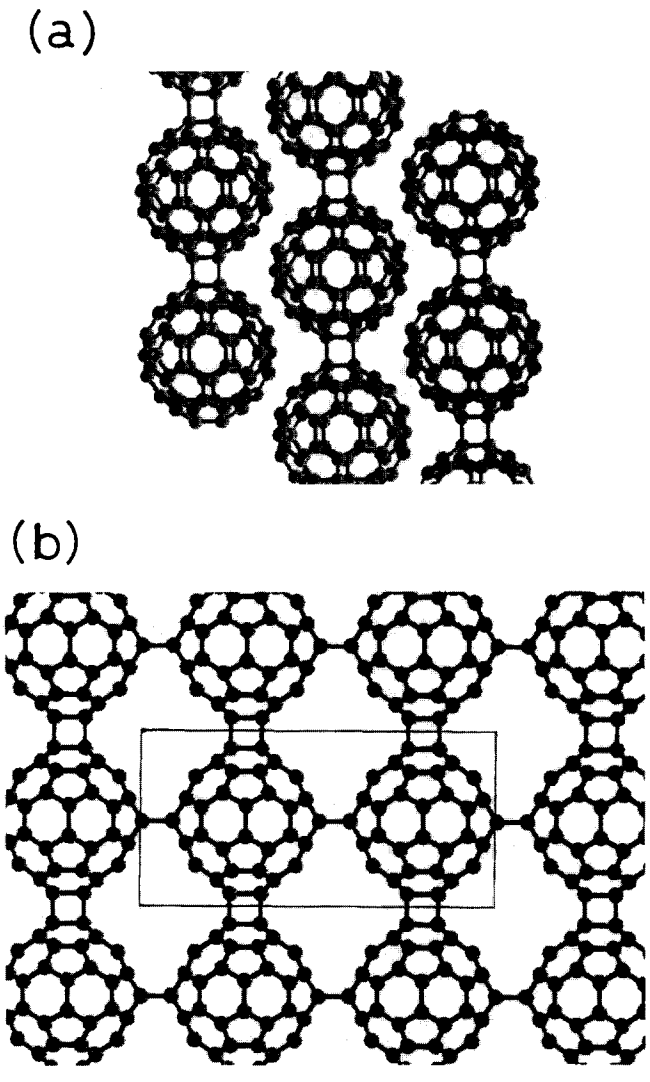

Figure 12 Energetically minimized models of (a) one-dimensionally and (b) three-dimensionally linked C_{60} crystals

is about 600 GPa in all directions. The idea has also been applied to cellulose. Starting from the structure of energetically minimized cellulose crystal, the three-dimensionally crosslinked cellulose crystal was constructed in which the OH and CH_2OH side groups are replaced by CH_2 groups. The Young's modulus along the main chain is about 250 GPa and those in the lateral directions are 130–200 GPa. These values should be compared with those of the highly anisotropic cellulose crystal: ca. 183 GPa along the chain axis, ca. 112 GPa in the sheet plane and ca. 13 GPa in the direction perpendicular to the sheet plane, calculated on the basis of the force-field parameters of Dreiding II[38]; or 168, 60 and 20 GPa, respectively, calculated by force constants adjusted to reproduce the vibrational spectral data[32].

The C_{60} molecule, buckminsterfullerene, is an electronically conjugated spherical molecule. We have tried to construct one-, two- or three-dimensionally crosslinked C_{60} crystals on the basis of the above-mentioned principle. A single C_{60} molecule was generated and energetically minimized in a simple cubic lattice. Then the molecules were linked covalently along one axis to

create a one-dimensional polymer crystal, which was found to be just the same model proposed for the polymerized C_{60} substance[40,41]. This one-dimensional polymer chain was further crosslinked into two-dimensional and three-dimensional network structures. This model was minimized energetically and the elastic constants were calculated based on the second derivative method. The obtained Young's modulus and bulk modulus (*BM*) are listed in *Table 3*. In *Figure 12* are shown the one- and three-dimensionally linked C_{60} network structures. The one-dimensional polymer has a modulus comparable to those of aromatic polyamide and polyester[1,2]. In the case of the three-dimensional network, the modulus is 150–180 GPa in all directions.

In this way, starting from conventional polymer substances, we can construct a variety of new polymer materials with three-dimensionally high elastic moduli through a very simple but quite useful crosslinking method. The crosslinked PA and PPP structures are interesting also in that they are three-dimensionally conjugated systems. Suitable doping of metal ions into these structures may give highly electrically conductive polymers in three dimensions. That is to say, we might have novel polymer materials with excellent mechanical and electrical properties, exceeding those of diamond crystal. At this stage, however, readers may notice that we now have one significant problem to solve. 'How can we actually synthesize these new materials?!'

REFERENCES

1 Tashiro, K. *Koubunshi Ronbunshu (Jpn. J. Polym. Sci. Tech.)* 1992, **49**, 711
2 Tashiro, K. *Progr. Polym. Sci.* 1993, **18**, 377
3 Tashiro, K., Nishimura, H. and Kobayashi, M. *Polym. Prepr. Jpn.* 1995, **44**, 3085
4 Tashiro, K., Kobayashi, M. and Yabuki, K. *Koubunshi Ronbunshu (Jpn J. Polym. Sci. Tech.)* 1994, **51**, 265
5 Tashiro, K., Kobayashi, M. and Yabuki, K. *Synth. Metals* 1995, **71**, 2102
6 Born, M. and Huang, K. 'Dynamical Theory of Crystal Lattice', Oxford University Press, London, 1954
7 Tashiro, K., Kobayashi, M. and Tadokoro, H. *Macromolecules* 1978, **11**, 908
8 Tashiro, K., Wu, G. and Kobayashi, M. *J. Polym. Sci. (B) Polym. Phys.* 1990, **28**, 2527
9 Tashiro, K., Minami, S., Wu, G. and Kobayashi, M. *J. Polym. Sci. (B) Polym. Phys.* 1992, **30**, 1143
10 Lacks, D. J. and Rutledge, G. C. *J. Phys. Chem.* 1994, **98**, 1222
11 Tashiro, K., Kobayashi, M. and Tadokoro, H. *Polym. J.* 1992, **24**, 899
12 Rutledge, G. C. and Suter, U. W. *Polymer* 1991, **32**, 2179
13 Parrinello, M. and Rahman, A. *J. Chem. Phys.* 1982, **76**, 2662
14 Tashiro, K. Kobayashi, M. and Tadokoro, H. *Macromolecules* 1978, **11**, 914
15 Miyasaka, K., Isomoto, K., Koganeya, K. and Ishikawa, K. *J. Polym. Sci., Polym. Phys. Edn.* 1980, **18**, 1047
16 Tashiro, K. and Tadokoro, H. *Macromolecules* 1981, **14**, 781
17 Wu, G., Tashiro, K. and Kobayashi, M. *Macromolecules* 1989, **22**, 758
18 Sawatari, C. and Matsuo, M. *Macromolecules* 1986, **19**, 2653
19 Kusanagi, H., Tadokoro, H., Chatani, Y. and Suehiro, K. *Macromolecules* 1977, **10**, 405
20 Tashiro, K., Kobayashi, M. and Tadokoro, H. *Macromolecules* 1977, **10**, 731
21 Nakame, K., Nishino, T., Hata, K. and Matsumoto, T. *Koubunshi Ronbunshu (Jpn. J. Polym. Sci. Tech.)* 1985, **42**, 361
22 Takahashi, Y., Kurumizawa, T., Kusanagi, H. and Tadokoro, H. *J. Polym. Sci., Polym. Phys. Edn.* 1978, **16**, 1999
23 Ii, T., Tashiro, K., Kobayashi, M. and Tadokoro, H. *Macromolecules* 1987, **20**, 347
24 Thistlewaite, T., Jakeways, R. and Ward, I. M. *Polymer* 1988, **29**, 61
25 Matsuo, M. and Sawatari, C. *Polym. J.* 1990, **22**, 518
26 Tashiro, K. and Kobayashi, M. *Macromolecules* 1991, **24**, 3706
27 Lenhert, P. G. and Adams, W. W. *Mater. Res. Soc. Symp. Proc.* 1989, **134**, 329
28 Wierschke, S. G., Shoemaker, J. R., Haaland, P. D., Pachter, R. and Adams, W. W. *Polymer* 1992, **33**, 3357
29 Tashiro, K. and Kobayashi, M. *Sen-i Gakkaishi* 1987, **24**, 3706
30 Sakurada, I. and Kaji, K. *J. Polym. Sci.* 1970, **31**, 57
31 Matsuo, M., Sawatari, C. and Imai, Y. *Macromolecules* 1990, **23**, 3266
32 Tashiro, K. and Kobayashi, M. *Polymer* 1991, **32**, 1516
33 Ito, T. *Polymer* 1982, **23**, 1412
34 Wu, G., Tashiro, K. and Kobayashi, M. *Macromolecules* 1989, **22**, 188
35 Tashiro, K., Kobayashi, M. and Tadokoro, H. *Polym. Eng. Sci.* 1994, **34**, 308
36 Tashiro, K. and Kobayashi, M. *Polym. Prepr. Jpn.* 1995, **44**, 714
37 Rappe, A. K., Casewit, C. J., Colwell, K. S. and Goddard, III, W. A. *J. Am. Chem. Soc.* 1992, **114**, 10024
38 Mayo, S. L., Olafson, B. D. and Goddard, III, W. A. *J. Phys. Chem.* 1990, **94**, 8897
39 Nakamae, K., Nishino, T. and Goto, Y. *Polym. Prepr. Jpn.* 1994, **43**, 1322
40 Rao, A. M., Ahou, P., Wang, K.-A., Hager, G. T., Holden, J. M., Wang, Y., Lee, W.-T., Bi, X.-X., Eklund, P. C., Cornett, D. S., Duncan, M. A. and Amster, I. J. *Science* 1993, **259**, 954
41 Zhao, Y. B., Poirier, D. M., Pechman, R. J. and Weaver, J. H. *Appl. Phys. Lett.* 1994, **64**, 577